ESTHER Shock Tube Diaphragm Project

Francisco Afonso

francisco.afonso@tecnico.ulisboa.pt

Instituto Superior Técnico, Universidade de Lisboa – Portugal

December 2019

This thesis shows the Sock Tube ESTHER diaphragms design, a partnership between ESA and Instituto de Plasmas e Fusão Nuclear of Instituto Superior Técnico.
This ESA project has as its object of study the re-entry of aircraft into the earth atmosphere and these diaphragms separate the combustion chamber that operates at extreme pressure levels from the shock tube.
The main objectives of this thesis are: 1) diaphragm sizing and notch geometry; 2) determination of the opening time of the diaphragms; 3) manufacturing options; 4) Design of some tube components.
This thesis arises from the research work developed at the IPFN which consisted in the determination of the diaphragm geometry.
In the analysis of the diaphragms, the conditions to which the diaphragm is subjected were verified and a structural analysis was performed through the Finite Element Method that allowed to verify the material to be used as well as the appropriate geometry for the diaphragms. In addition to the design of the diaphragms, some subsets of the shock tube were also designed and some modifications that were necessary during the course of the project.
In conclusion, we present the diaphragm geometry and the shock tube in their final version in terms of design and manufacture.

Keywords: Diaphragm, Shock Tube, groove geometry, Finite Element Analysis, pressure, ESA

1. Descritive Memory

1.1. Motivation

The objective of this work is to determine the entire dimension of a diaphragm that separates a combustion chamber from a shock tube. The diaphragm is a round plate embedded in a support, with indentation that aims to open at a predetermined burst pressure in form of petals so that the flow occurs without swirling. This equipment is located in the Nuclear and Technological Campus of the Institute of Nuclear Fusion and Plasma Institute, which has as its main objective the projection of one spacecraft and planetary exploration, funded by European Space Agency (ESA).

The main goals are, firstly, to determine the thickness of the plate and from there, knowing that there should be two indentations in the exposed area, determine

the depth of the notch and the opening angle Although there are three service pressures, the study focuses on the critical service pressure of 600 bar.

Similar tests were performed, however, the shock tubes, beside being smaller, the material used was copper that had the expected behavior under the conditions to which it was subjected. In this work the challenge is to try to get the same model but now using steel, which is a challenge to the service pressures that ESTHER will operate. Along with the diaphragm sizing, in this work, the shock tube equipment was improved to find solutions that would guarantee the tube stability in other sections, as well as the sizing and analysis of options in the diaphragm supports

1.2. ESTHER Shock Tube Description

The shock tube consists of a combustion chamber, where a mixture of He gases, at a initial pressure up to 100 bar and a final pressure of 600 bar ignites through a high intensity leisure beam. The plant operates in deflagration (subsonic combustion), however detonations (supersonic combustion) may occasionally occur, providing transient pressures of the order of 2.4 Kbar. The combustion chamber is made of low carbon superduplex steel, which has high mechanical strength and is indicated for no reaction with hydrogen. The chamber has an internal diameter of 200 mm. The diaphragm, designed to open at a predetermined pressure, connects the combustion chamber to an intermediate compression tube. This tube is filled by He gas at pressures of about 0.01-1 bar. The shock wave propagates in this section, leading to transient reflected pressures of 70 bar. The end sections of the tube are made of duplex stainless steel, which also has a low carbon composition. The compression tube section has an internal diameter of 130 mm and is connected to the shock tube test section by a new diaphragm also designed to open at a predetermined pressure. This new pipe section is filled by a test gas at pressures of about 0.1 mbar. The shock wave propagates in this section at speeds that may exceed 10 km/s, leading to transient reflected pressures of not more than 20 bar. The tube is made by duplex stainless steel. This section has an internal diameter of 80 mm.

Along the pipe are pressure sensors that detect the increase pressure in the shock wave mat. This allows the development of a firing system by initiating high-speed (10-100MHz) spectroscopic measurements of the emitted and absorbed radiation in the wake of the wave depending on the time in the test section windows (25 mm in diameter).

The discharge tank recovers all gases flowing in the wake of the wave. The liquid phase is drained, while the remaining contaminated mixture is evacuated by the pumping system, which allows the tube to be opened for diaphragm cleaning and replacement operations.

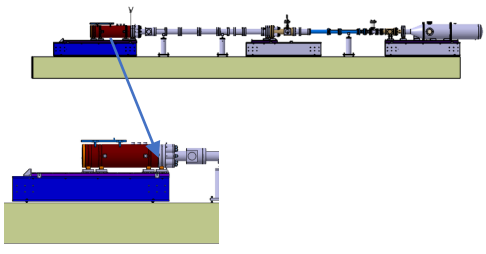

Fig. 1 Shock Tube ESTHER and combustion chamber detail

1.3. Diphragms supports

For retention geometry two notches with 1 mm height (H) were adopted, with different positioning in order to promote the material creep without the critical situation of pure cutting. This option is justified by the impossibility of precision of this manufacturing company.

Given the service life of the part and the number of loading cycles to which it will be exposed, it was also chosen to consider curvature at the end of the notch in order to provide greater fatigue strength. This type of option also prevents such a high local stress concentration. This consideration was taken in accordance with the results set forth in the following sections, since at the time of opening, the ring-membrane contact zone is one of the areas with the highest stress concentration and may even be considered one of the most sensitive areas. Therefore, special attention should be given to the fact that one of the main risks of the experiment is the pure cut of the petal which could break and damage the entire tube due to the high flow that occurs in it.

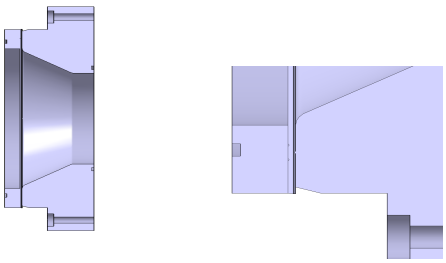

Fig. 2 Diaphragm supports and notches detail

1.4. Combustion Chamber

The connection between the combustion chamber and the compression tube part CT1 was initially designed with a standardized M52 bolt which would have a hydraulic force to prevent the bolt from showing tensile forces. When the project was carried out, it was taken into account that in another phase, the camera could be connected to part ST1.

Due to a manufacturing error, it was necessary to manufacture new screws.

In a first approach, it was proposed to drill the holes at M60, however, this would not be feasible since the hydraulics were already purchased and it would not be possible to use an M60 rod.

In order to correct the manufacturing error, a final solution was found which consisted of drilling the camera holes at M60 and drilling the holes of part CT1 and ST1 through M54. In this way, the use of the hydraulics already acquired would be made possible. A rod like the one shown in figure 5 was then designed, which starts at M60 until the end of the chamber bore, and then passes at M52, presenting a transition of about 10 cm, which ensures no stress concentration in the change of diameter that could under fatigue lead to its breakage.

AISI 630 steel was adopted with a hardening temperature of 495 ° C, which has a yield strength of 1070 MPa. Initially, according to the above-mentioned bibliography, another steel with a yield strength much higher than this steel had been selected, however the company responsible for the manufacture of the screws had no way of acquiring it and so the closest solution presented to us and which would become efficient in order not to lower the resistance class was that corresponding to AISI 630.

The figure 3 illustrates the camera already with the new screws in position.

Fig. 3 Final screws

1.5. Pressure

To experimentally validate the ESTHER design combustion chamber, a prototype combustion chamber was designed by A.Chickhaoui and JM-Félio of the Université de Provence, with an inner diameter of 80 mm, an outer diameter of 240 mm and a length 600 mm for a total volume of 3 liters. The chamber features a gas inlet and outlet, two wiring inlets, one pressure gauge inlet and two additional unused inputs. The ignition was made through a hot wire system placed in two small copper brackets that are inserted into the wire holder connectors, with the electric wire being placed on the symmetry axis of the cylinder. Access for maintenance and cleaning operations was made through one of the end caps and the cover is always kept closed as long as the gas outlet pipe is connected to it.

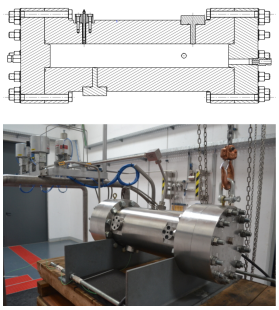

Fig. 4 (a) Technical drawing of chamber (b) chamber after manufacturing

Through this prototype it was possible to select the pressure profile that best approximates the expected profile in the project combustion chamber, corresponding to test 177 and thus insert it as a condition in the Finite Element simulation for a better approximation of reality, once Considering a constant pressure over time would be a far cry from reality since it is not constant over time as shown in the pressure-time graph represented in figure 5:

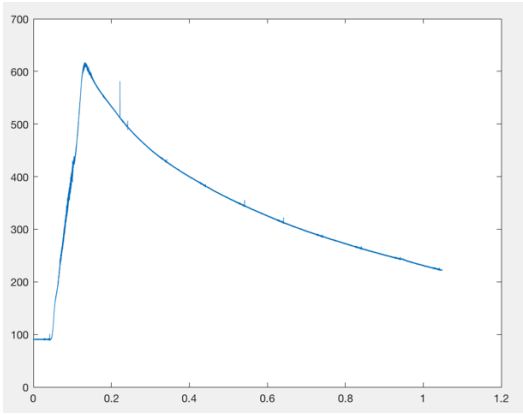

Fig. 5 Pressure (bar) vs time (ms) profile

It can be seen from the graph that the pressure peak is about 0.13 ms, and according to the design safety coefficient the opening of the diaphragm should be 580 bar corresponding to the approximate time of 0.124 ms.

1.6. Temperature

In the combustion chamber the combustion of hydrogen, oxygen and helium occurs, obtaining as products helium and water. The mixture is considered a supercritical fluid that is distinguished in two phases, one of supercritical liquid and one of supercritical gas. However, given the operating temperature and pressure, the present phase is mostly gaseous.

We have as critical temperatures:

Table 1 Critical Temperatures

Reagents	Critical Temperature (K)
H_2	33,2
He	5,19
O_2	154,6
Products	**Critical Temperature (K)**
He	5,19
H_2O	647,096

As temperatures are much higher than critical temperatures, we are dealing with a superfluid gas, and in this case, and according to the reference [14] in cases of injection and combustion the law of perfect gases is applicable in particularly in the camera's range of service.

From the pressure plot as a function of time, it is known that the pressure peak occurs at 640 bar and knowing from pump measurements the temperature at the maximum pressure point of 2800 K using the Gas Law Perfect in the form PV = nRT, we can formulate a temperature model of the type: T (t) = K * p (t) where, K, represents a constant which according to known data at the maximum pressure point is given by:

$$K = \frac{T_{max}}{p_{max}} = \frac{2800}{640} \quad (1)$$

From the above model we obtained a temperature profile, as a function of time T (t), represented in figure 6 that will allow us a more careful analysis in the finite element simulations to be performed.

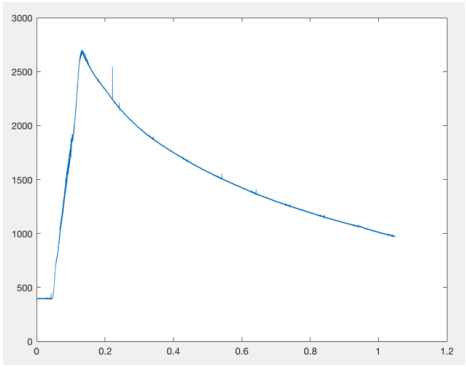

Fig. 6 Temperature (K) vs time (ms) profile

1.7. Project Requirements

I) The material used in the pipe should contain as little carbon content as possible to ensure no reaction with the mixture.

II) The manufacturing process should ensure the desired geometric integrity and should be low cost.

III) The opening time of the diaphragm should be close to the theoretical value.

IV) The support structure of the diaphragms should prevent the diaphragms from slipping when opening them.

V) Diaphragms should be made of low cost steel

1.8. Project Security

1.8.1. Inertial Impact Structure

The structure was structurally constructed with standard I-profile beams and two crates, which have a lid to allow them to be opened and the weight placed on them to be removed, thus facilitating their transport. Each crate has a weight of 1500kg to absorb all the shock energy.

This structure was designed according to the law of kinetic energy transfer to bodies of equal mass. After transferring the kinetic

energy from the chamber to the structure, it eventually falls and the structure moves, eventually losing all of its energy once the roughness on the floor causes enough friction for the structure to lose movement.
The structure is shown in figure 7 schematically.

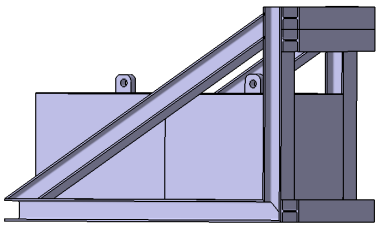

Fig. 7 Inertial Impact structure

1.8.2. Vacum pump suspension

The concept mechanism that was conceived consists first of all of a massive block that puts the structure as a whole in equilibrium, since it was not in equilibrium statistically because of the unilateral vacuum mechanism. To suspend the bomb, a mechanism was thought similar to the scales used in the 19th century, as illustrated in figure 8.

Fig. 8 Inspiration model to the mechanism

Conceptual scheme is presented in figure 9:

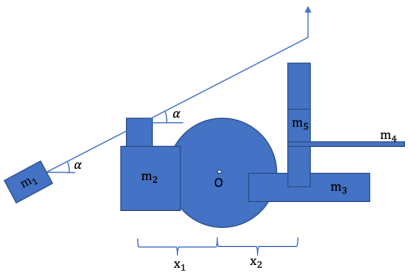

Fig. 9 Schematic model to the static equilibrium

The figure 10 presents the final version of the geometry that converged to the proposed mechanism and already dimensioned.
As mentioned earlier this geometry is a very versatile solution to future tube changes such as a different pump with a different weight. This makes it possible for the tube to be stable when it is in operation and has allowed the connecting bolts to cease to be subject to moments that could compromise the correct and safe operation of the tube.

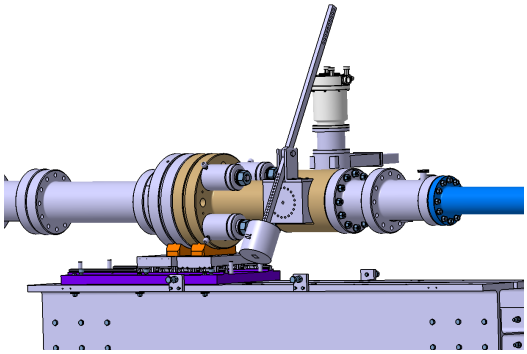

Fig. 10 Final desing to the mechanism

1.9. AISI 304L Tension Test

The test was performed at the Materials Laboratory of the Mechanical Engineering Department of the Higher Technical Institute using an INSTRON 3369 testing machine and a specimen according to 304L steel as previously specified, as well as a static type strain gauge. The specimen was placed in the machine fasteners and the strain gauge was placed in the middle of the exposed

portion of the specimen in order to increase the sensitivity of the strain gauge to low deformations throughout the process.

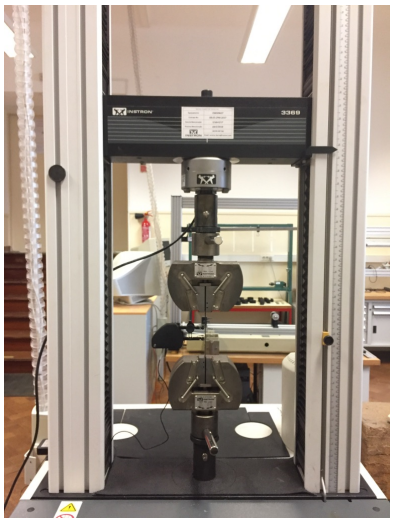

Fig. 11 Tensile test machine

After data processing a set of points was obtained from which the following graph was elaborated that allows us to obtain the mechanical properties of the material:

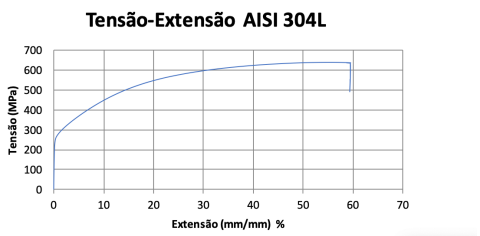

Fig. 12 AISI 304L Stress-Strain Profile

The mechanical properties of the material obtained after graph analysis are summarized in the table 2:

Table 2 AISI 304 L mechanical properties

Property	E (GPa)	σ_y(MPa)	UTS (MPa)	ε_{max}
Value	161,4	255,4	645,7	0,54748

2.Simulation

2.1. Simulation Results

According to this geometry:

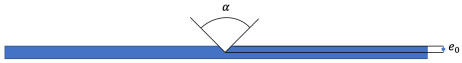

Fig. 13 Groove scheme

We have this possible variable parameters:

Table 3 Variable parameters

Angle α (°)	Depth e_0 (mm)
45	1
60	1
60	0.5
90	1

In terms of the simulation will be considered the follow components with the respective mesh:

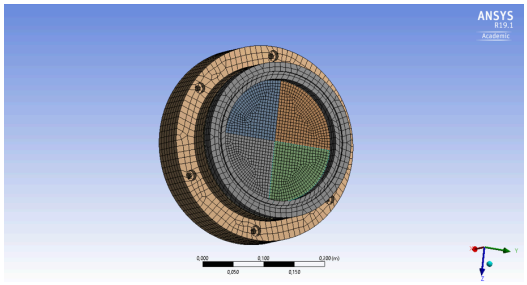

Fig. 14 Mesh

And the contact relations:

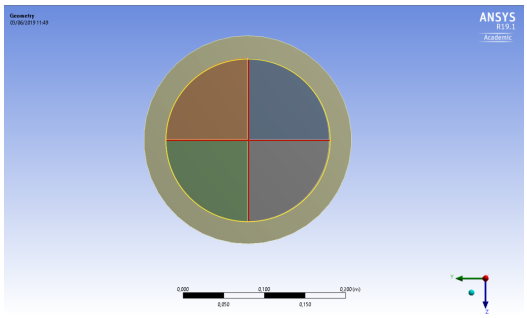

Fig. 15 Contact Relations

The membrane was divided into five different bodies to which the relationship between them is attributed, outlined in red and yellow, with the yellow line representing bonded interaction and the red line representing rough.

After analyzing the simulations we have:

Table 4 Simulation Results

Ângle, α (°)	Depth,e_0 (mm)	Opening Time (s)
45	1	$2{,}16 \cdot 10^{-4}$
60	1	$1{,}24 \cdot 10^{-4}$
60	0.5	$1{,}61 \cdot 10^{-4}$
90	1	$2{,}04 \cdot 10^{-4}$

The optimum opening time is before the pressure peak within the combustion chamber is reached, and the optimum opening pressure is about 580 bar. It was from this same analysis that we arrived at the final diaphragm geometry which corresponds to the geometry that has a notch angle of 60 ° and a depth of 1mm.

From the obtained results it is noteworthy that for an angle of 45 ° and a depth of 1mm it is observed a very sharp straining of the petals that significantly reduce their thickness and that in limit situations they may detach from the embedded zone and cause damage along the risk that should be mitigated to the maximum.

Below are some simulation images concerning the final diaphragm geometry.

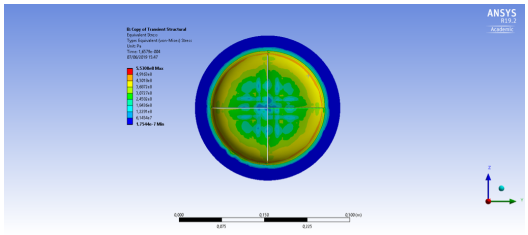

Fig. 16 von-Mises Results

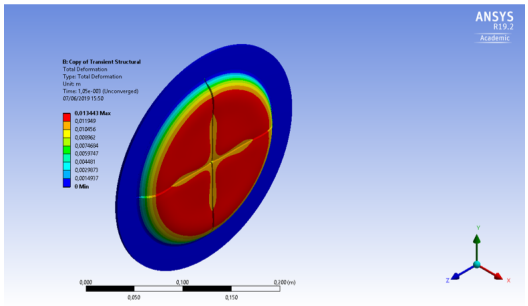

Fig. 17 Deformation Results

2.2. Manufacturing Method

Given the sensitivity of the type of tests that will be performed with the diaphragm and its design, electro-erosion machine in direct polarity conditions has been selected as the ideal process for obtaining accurate results. As noted in previous sections, given the high number of diaphragms that will be used over the ESTHER's estimated lifetime, the electron erosion process is not only costly in monetary terms but it is inefficient to meet the manufacturing need.

In a first approach to this problem a prototype has been suggested which allows the manufacture of the diaphragms in the easy-to-handle laboratory itself and which requires short manufacturing times.

The proposal presented in figure 8, is a scheme that was proposed to those responsible for ESTHER.

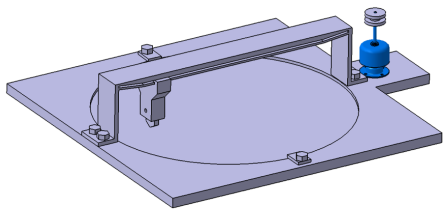

Fig. 18 Manufacturing machine concept

The economically viable process which would satisfy the need for components to be fabricated would be an end mill. This solution is the one that will be used when manufacturing the diaphragms, however, it is emphasized that it does not guarantee the necessary precision and may affect the result to be obtained in the experimental tests.

3. Conclusions

This document presents the design of the diaphragms and some components of the ESTHER shock tube. In this project, the

numerical analysis using the Finite Element Method, MEF (numerical method) was used to determine the parameters under study in the case of the diaphragm using the transient-structural analysis that allows to predict the behavior of the object under study after rupture.

Being in the presence of a superfluid, the theoretical value for the validation of the geometric parameters is the time until combustion occurs, a value that was obtained experimentally in a prototype chamber. The values obtained for the expected opening time, taking into account all the simplifications taken, are in agreement with what was obtained experimentally by which the theory is validated. The FEM is a method that gives very detailed and very accurate results, but it also requires critical sense from those who use the method in order to interpret the results obtained. The entire structure is oversized for safety and precision.

The final geometry arrived at corresponds to an opening angle of 60 ° and a depth of 1 mm. The diaphragm will have two tears along a length of 200 mm corresponding to the diameter of the diaphragm area exposed to the flow.

Note that the indentations should be made at 45 ° in relation to the machining direction of the plate as it is the preferred direction for shear stresses.

Some shock tube components have also been sized and designed.

Future studies could optimize and automate the parameter setting method so that different materials can be used in the diaphragm as well as the option of placing more than two notches. Although the price of the material used is low, it is a new challenge to try to use a new material.

Regarding the method of manufacturing the diaphragms, it was decided to purchase a CNC that allowed the manufacture of the diaphragms in their own facilities in order to reduce their cost of manufacture, although this alternative was not ideal regarding the sensitivity of the study.

As ESA is a worldwide reference in aerospace research and IPFN a reference in research in Portugal and worldwide, it was a privilege to be able to participate in this research that enriched me as an engineer because I had the possibility to face a very challenging project that provided me with a critical analysis and on the other hand, it allowed me to contact with manufacturing errors and to contact with the factory area that in a university context would not be possible before finishing a college degree.

4. References

[1] Yamaki, Y. Rocker, R.J. Experimental Investigation of circular flat, grooved and plain steel diaphragms bursting into a 30.5-centimeter-square section, 1972

[2] Rodrigues J., Martins P.; Tecnologia Mecânica Vol I – Fundamentos Teóricos; Escolar Editora, 2ª Edição;

[3] R.W. Henderson; AN ANALYTICAL METHOD FOR DESIGN OF SCORED RUPTURE DIAPHRAGMS FOR USE IN SHOCK AND GUN TUNNELS, Technical Memorandum, March 1967;

[4] Drewry and Walenta in Drewry, J.E.; and Walenta, Z.A.: Determination of Diaphragm

Opening-Times and Use of a Diaphragm Particle Traps in Hypersonic Shock Tube. UTIAS Tech. Note No.90, Inst Aerosp Studies, Univ of Toronto, June1965;

[5]Sympson, C.J.S.M.; Chandler, T.R.D.; and Bridgeman, K.B.: Measurement of Opening Times of Diaphragms in a Shock Trajectories. NPL Aero Rep. 1194, Brit. A.R.C., May 1966;

[6] website matweb.com, consultado em Julho, 2019;

[7] ASTM E8/E8M -09 Standard Test Methods for Tension Testing of Metallic Materials;

[8] https://upload.wikimedia.org/wikipedia/commons/0/0c/Stress_v_strain_Aluminum_2.png, consultado no dia 4/5/2019;

[9] http://www.onzedinheiros.lel.br/peca.asp?ID=1541411&ctd=8&tot=89&tipo=6, consultado no dia 22/06/2019;

[10] Edwards D.G.: The Bursting Pressure of Metal Diaphragms in Square Section Shock Tubes. Department of Mechanical Engineering, University of Surrey, January 1970;

[11] Amstrong A.J.; Watson R.: Bursting Characteristics of Thin Metal Diaphragms in Shock Tubes;

[12] Wilson J.: A Rough Calculation of Shock-Tube Diaphragm Opening Times, Royal Aircraft Establishment, January, 1963

[13] Yamaki Yoshio; Rooker R.J.: Experimental Investigation of Circular, Flat, Grooved and Plain Steel Diaphragms Bursting into

[14] https://en.wikipedia.org/wiki/Critical_point_(thermodynamics), consultado no dia 15/06/2019

[15] Hamrock Bernard, Jacobson Bo, Schimid Steven: Fundamentals of Machine Elements – Second edition, 2004 McGraw-Hill ISBN 978-007-12579